Improving Reduced-Order Building Modeling: Integration of Occupant Patterns for Reducing Energy Consumption

Jovana Kovačević
Institute for Automation and Applied Informatics
Karlsruhe Institute of Technology
Germany
jovana.kovacevic@kit.edu

Chang Li
Institute for Automation and Applied Informatics
Karlsruhe Institute of Technology
Germany
chang.li@kit.edu

Kevin Förderer
Institute for Automation and Applied Informatics
Karlsruhe Institute of Technology
Germany
kevin.foerderer@kit.edu

Hüseyin K. Çakmak
Institute for Automation and Applied Informatics
Karlsruhe Institute of Technology
Germany
hueseyin.cakmak@kit.edu

Veit Hagenmeyer
Institute for Automation and Applied Informatics
Karlsruhe Institute of Technology
Germany
veit.hagenmeyer@kit.edu

ABSTRACT

The accuracy in reduced-order building models affects prediction of energy consumption and indoor air temperature through the quality of control strategies in buildings. The parameter identification in grey-box thermal building models can be influenced by different disturbances such as ambient temperature, solar radiation and activities related to occupant behavior. To tackle these challenges, in this paper, we propose a novel ensemble model that distinguishes the parameter estimation on two different periods: working days and weekend, to advance the integration of different occupant behavior patterns. The ensemble model is developed based on a decentralized multi-zone building model and measurement data to investigate the robustness of the proposed model. We compare and discuss the results obtained from the proposed model with the classic model identification approach to quantify the performance of the ensemble model. In contrast to the classic model, in which the difference in transmission heat energy through external walls and roof to the measurement data over five experimental weeks is 278 kWh, the proposed novel ensemble forecast method outperforms it with only 132 kWh. With the proposed model we obtain a more precise forecasting of indoor air temperature in all considered zones, which has the potential to enhance energy reduction in buildings using model predictive control strategies.

CCS CONCEPTS

• **Computing methodologies** → **Model verification and validation**; • **Hardware** → **Temperature simulation and estimation**.

KEYWORDS

grey-box, occupant behavior, reduced-order modeling, thermal building model, temperature estimation

ACM Reference Format:
Jovana Kovačević, Chang Li, Kevin Förderer, Hüseyin K. Çakmak, and Veit Hagenmeyer. 2024. Improving Reduced-Order Building Modeling: Integration of Occupant Patterns for Reducing Energy Consumption. In *The 15th ACM International Conference on Future and Sustainable Energy Systems (E-Energy '24), June 04–07, 2024, Singapore, Singapore.* ACM, New York, NY, USA, 11 pages. https://doi.org/10.1145/3632775.3662163

E-Energy '24, June 04–07, 2024, Singapore, Singapore

ACM ISBN 979-8-4007-0480-2/24/06
https://doi.org/10.1145/3632775.3662163

1 INTRODUCTION

Building energy consumption has increased rapidly in recent years, and its share accounts for 30 % of global energy consumption and 26 % of energy-related emissions [21]. Thus, great potential for energy reduction lies in the advancement of heating, ventilation, and cooling (HVAC) systems as they account for a large share of energy consumption. To achieve energy-efficient coordination of HVAC systems in buildings, accurate control strategies are necessary, where model predictive control (MPC) gains popularity [7, 24, 30]. Besides optimization of HVAC systems, MPC can also consider demand response (DR) and occupants thermal satisfaction (OTS), along with grid flexibility services [13]. However, the main difficulty of practical implementation of MPC is an accurate model development [9], where the accuracy of models has a significant impact on the control performance.

Typically, thermal building models used in MPC are divided into three main categories: white-, black- and grey-box models [5]. White-box modeling is a physics-based modeling approach that requires a knowledge of building properties such as the geometry of the building, heat conduction, and material types [5]. White-box models can provide an understanding of the relationship between different energy components in buildings. However, these models are usually difficult to develop and calibrate [2]. Since these models involve many equations and nonlinear characteristics, their implementation in model-based control strategies is difficult [13]. In contrast, the black-box modeling approach is purely based on

data-driven methods, and the prediction is obtained by mapping input and output data. The physical structure is not considered and the forecasting highly depends on training data [28]. The third approach is grey-box modeling, which was developed to overcome the disadvantages of white- and black-box approaches [1]. Grey-box models have a physical structure, for which parameter identification can be done by using a forward or inverse approach. The forward approach is based directly on physical models for parameter identification, and the inverse approach uses data-driven methods, e.g. curve-fitting [28]. Grey-box thermal building models can achieve high accuracy with additional benefits as simplicity and low computational costs. However, the development of data-driven grey-box models requires involving knowledge of both, the equation-based structure and data-driven methods for parameter identification. Nevertheless, their prediction highly depends on the accuracy and quality of the underlying measurement data and the accuracy of parameter estimation [5]. Besides model-based control strategies, grey-box thermal building models have a wide range of usage in different areas such as prediction of energy consumption and evaluation of energy performance of the buildings and districts [4]. When it comes to MPC, by increasing the complexity of the thermal building model structure, e.g. multi-zone models, the accuracy of the model increases and OTS can be considered in more detail. Conversely, the overall computational demand of MPC increases. Hence, a suitable trade-off between the precision and simplicity of the grey-box models has to be found.

The performance of grey-box thermal building models plays a crucial role in the prediction of effective building energy control. To advance the robustness of the grey-box models to occupant patterns, which affect significantly indoor air temperature forecast, this paper introduces a novel grey-box thermal building model structure consisting of two identified models: the working day model and the weekend model. The investigated model prediction spans five weeks and is compared with the prediction of the classically identified thermal building model, such as in [14, 18], where the whole week is used for identification. The parameters are identified based on measured data of a real office building, where occupants have a stochastic influence on indoor air temperature. For analysis and testing of the introduced models, the Living Lab Energy Campus (LLEC) facility as part of the Real Laboratory Energy Lab 2.0 [17], located at Karlsruhe Institute of Technology (KIT) is utilized.

The rest of this paper is organized as follows: Section 2 presents related work in the grey-box thermal building modeling research area. Section 3 introduces the model structure and a proposed methodology for parameter identification in grey-box models. Sections 4 and 5 show the obtained experimental results and the evaluation of the proposed methodology. Sections 6 and 7 discuss the proposed methodology and conclude this paper.

2 RELATED WORK

Several studies point out challenges in the grey-box thermal building modeling approach: [6, 8, 28]. Li et al. [28] identify the grey-box model structure itself and its creation process as being vague. They point out that suitable applications of grey-box models are obscure, although most studies use grey-box models for control and optimization of energy consumption in buildings, heat dynamics estimation, evaluation of energy consumption on the building, district, or city level, and building-grid integration. The correct labeling is also unclear since grey-box models can represent one component, such as a window or wall, one zone, or multiple zones. Broholt et al. [8] point out the challenge of grey-box models prediction robustness when models are identified on certain months and used for the forecast of the thermal behavior for the rest of the year. The robustness of grey- and black-box models are compared, whereas results show a slightly better prediction quality of grey-box models. Belazi et al. [6] also address the challenge of grey-box model robustness on weather data. They investigate the effect of input uncertainties: occupancy behavior, and parameters related to the building envelope on the energy performance. The main finding is the greater impact of occupancy behavior in hot climates, while in cold climates, parameters related to the building envelope come to the fore.

Table 1 lists several studies that investigated improvements of grey-box thermal building models. Gray et al. [16] and Cui et al. [11] examine simplified grey-box thermal building models in combination with black-box models for an improved forecasting. In the former study, the combination of simplified grey-box models with gaussian process (GP) modeling is compared with pure grey-box and black-box models. The second study compares grey-box models with integration of different machine learning algorithms, where it is stated that the combination of grey-box models and extreme gradient boosting (XBG) gives a most favorable performance. On the other hand, Michalak et al. [29] use a time-variant state-space system to achieve improvement of grey-box thermal building models. They use simulation data to update the parameters of the grey-box model hourly. Several studies compare different structures of the grey-box thermal building models, aiming to find the most performable model [3, 4, 18, 19, 26]. Bacher et al. analyze a method, called forward model selection strategy, for the identification and selection of an appropriate grey-box model structure. The complexity of the model structure is increased iteratively based on physical knowledge, whereas the method enables the selection of a suitable model structure with an appropriate complexity level. Baasch et al. [3] investigate the robustness of different grey- and black-box model structures towards foreign building properties (FBP), where deep learning methods give the most accurate and robust results. Harb et al. [18] compare 1R1C, 3R2C, 4R2C and 8R3C models for the prediction of indoor air temperature in the building with real occupants, where the 4R2C model has shown the most favorable performance. Klanatsky et al. [26] propose the integration of the large heat accumulating medium (LHAM) and large glass façades with external shading into the grey-box thermal building model structures. They compare various grey-box model structures, where the best model structure (3R3C) achieves a mean absolute error of 0.25 °C over the year (OTY) simulation. Besides the identification period, they introduce a startup period, which leads the model to a realistic state with plausible variables. The subsequent identification period assists in finding the best fit across the identification data set. With these, the prediction is examined for a time span of 24 hours by investigating the simulation time step, startup phase duration and training phase duration. Hedegaard et al. [19] compare parameters of thermal characteristics of the buildings obtained by calculation methods from standards and parameters estimated

Table 1: Studies related to improvements of grey-box modeling approach

Research	Method	Type of data	Id. Period	Val. period	Error of the best forecast
Gray et al. [16]	Simplified Grey-Box Model with GP	Simulation	1-4 weeks	weekly updated	RMSE = 0.2 OTY
Cui et al. [11]	Grey-Box + XGB	Real	~ 25 days	~ 17 days	RMSE = 0.641
Michalak et al. [29]	Time-Variant State-Space System	Simulation	N/A	hourly	RMSE = 0.5-0.8 OTY
Harb et al. [18]	Comparison (best 4R2C)	Real	26 days	8 weeks	RMSE = 0.2
Frahm et al. [14]	Minimalistic 4R3C	Real	13 days	13 days	RMSE = 0.705
Klanatsky et al. [26]	LHAM and Large Glass Façades with External Shading	Real	2-4 weeks	daily/weekly updated	MAE = 0.25 OTY
Frahm et al. [15]	Multi-Zone with OB: Weekend and Working Day Prediction	Real Real	2 days 5 days	2 days 5 days	RMSE = 0.36 RMSE = 0.85
Baasch et al. [3]	Robustness of the Grey- and Black-Box Models against FBP	Simulation	7 days	7 days	MAE = 0.34
Zhang et al. [32]	Improving Solar Heat Gain Dynamics in Grey-Box Models	Real	7 and 8 days	7 and 8 days	N/A
Bacher et al. [4]	Forward Model Selection Strategy	Real	28 days	N/A	N/A

using an inverse approach. Frahm et al. [14] propose a minimalistic 4R3C grey-box model for the prediction of the thermal response of an occupied building. It is stated that the error increases for the weekend forecasts due to the change of occupancy patterns. Coffman et al. [10] consider heat gains from occupants as an additional state to the 2R2C thermal building network, with the hypothesis that the occupant behavior patterns are constant throughout time. On the other hand, Zhang et al. [32] pointed out that in literature solar heat gains in grey-box models are simplified, which can lead to poor forecasting. They investigated and discussed advancements in dynamic solar gains, to fill this gap.

One difficulty of grey-box thermal building models is the integration of Occupants' behavior (OB) into the models, to achieve better forecasts. OB determines not only the interaction of the occupants with energy control systems and building components such as windows and lighting, but also the heat emitted by the occupants. Due to its complexity and since it is not well understood, OB is often simplified in energy building models [20]. Several studies already investigated the integration of OB into grey-box models [10, 14, 18, 29]. In a comparative study, Frahm et al. [15] investigate the impact of identification periods (occupied vs. unoccupied building) and conclude that these have a greater impact on the forecast than the structure of the model and algorithms. The change in patterns, i.e. impact of occupants, such as presence during working hours and absence during the weekends in commercial buildings, influences the grey-box thermal building model forecast by increasing the forecast error. Time-invariant state-space systems can not predict well such time-variant influences of OB. In order to achieve more precise grey-box thermal building models, there is a need to investigate different OB patterns and to separate their impact in different time-invariant state-space models. To address these research gaps, we propose a new method for the identification of grey-box models in order to improve time-invariant grey-box models of real-world buildings with occupants.

3 METHODOLOGY

The inverse grey-box building modeling approach is a combination of the physical structure and a data-driven approach for parameter identification [28], which we define as predefined model structure (PMS). Usually, it is called RC building modeling, where similar to an electrical circuit, electrical resistance (R element) in the grey-box thermal building model represents thermal resistance between corresponding thermal nodes, and capacitance (C element) is the heat capacity of the thermal node [13]. The number of heat capacitors defines the number of states that a grey-box model has. Besides ambient temperature and solar radiation, activities related to the occupants also have a great impact on the building energy performance [20]. Integrating the impact of occupant behavior patterns into reduced-order building models is not a straightforward task. Since occupant behavior greatly impacts indoor air temperature, it needs to be well investigated to be integrated into the model, thus preserving the data privacy of the occupants.

3.1 Model structure

To face the issue of the thermal building model's robustness to occupant-related heat load, the model structure is defined as follows:

$$C_{w,j}\frac{\mathrm{d}T_{w,j}}{\mathrm{d}t} = \frac{2(T_{i,j} - T_{w,j})}{R_{w,j}} + \frac{2(T_a - T_{w,j})}{R_{w,j}} \tag{1}$$

$$C_i \frac{\mathrm{d}T_{i,j}}{\mathrm{d}t} = \frac{2(T_{w,j} - T_{i,j})}{R_{w,j}} + \frac{(T_a - T_{i,j})}{R_{inf,j}} + \frac{T_{m,j} - T_{i,j}}{R_{m,j}} + q_{conv,j} + A_{s,j}G_s + q_{ig,j} \tag{2}$$

$$C_{m,j} \frac{\mathrm{d}T_{m,j}}{\mathrm{d}t} = \frac{(T_{i,j} - T_{m,j})}{R_{m,j}} + q_{rad,j} \tag{3}$$

$$\frac{\mathrm{d}q_{ig,j}}{\mathrm{d}t} = 0 \tag{4}$$

where index $j = (1, 2, ..., n)$ denotes the corresponding room and n denotes the number of rooms. $T_{w,j}$ represents the temperature of the wall and $T_{i,j}$ is the indoor air temperature. Moreover, $T_{m,j}$ is the temperature of the large heat accumulating medium (LHAM). All three of them are presented in °C, whereas $q_{ig,j}$ [W] denotes occupant-related heat load that impacts indoor air temperature. The $C_{w,j}$, $C_{i,j}$ and $C_{m,j}$ with corresponding unit [J/°C] are the thermal capacitance of the wall, the inner part of the wall and the large heat accumulating medium, respectively. The large heat-accumulating medium represents building components with slow thermal dynamics, e.g. roof, floors, inner concrete cores, etc. The thermal resistance $R_{w,j}$ is the thermal resistance against heat transfer between ambient air and indoor air, $R_{m,j}$ between large heat accumulating medium and indoor air, whereas $R_{inf,j}$ is infiltration resistance. All resistances are presented in [°C/W]. The input vector has the following form:

$$\mathbf{u}_j = [T_a \quad q_{h,j} \quad G_s]^T \tag{5}$$

where the first element represents ambient temperature in °C, the second heat flow from the heat pump in [W] and the latter solar radiation in [W/m^{-2}], whereas $A_{s,j}$ [m^2] in Equation (2) is solar heat gain factor. The heat flow is produced by the ground source heat pump, and the measured values are for the whole experimental building. Therefore, the heat flow per room is estimated based on ratio η of the room volume V_j to the sum of all room volumes $\sum_j^n V_j$:

$$q_{h,j} = \eta q_h \rightarrow \eta = \frac{V_j}{\sum_j^n V_j} \tag{6}$$

We assume the share of heat flow as 80 % of convective heat $q_{conv,j}$ and 20 % of radiant heat $q_{rad,j}$ as discussed in [22].

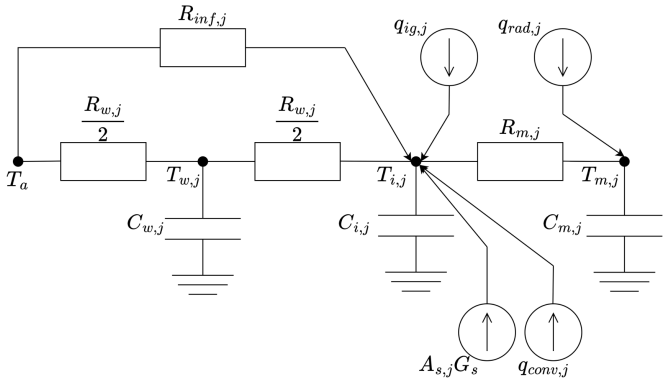

Figure 1: Predefined model structure of proposed grey-box thermal building model.

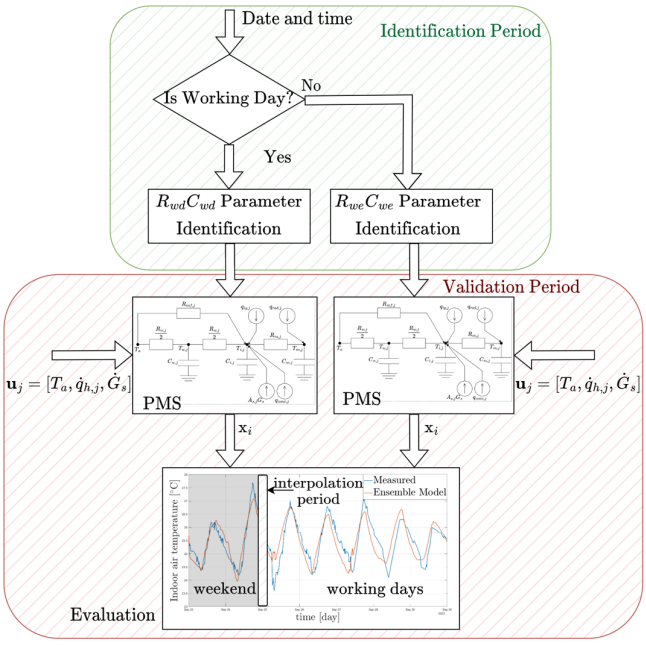

Figure 2: Methodology of the identification and validation process in ensemble model.

The RC representation of the thermal building model is shown in Figure 1. Originally, the model has three states $T_{w,j}$, $T_{i,j}$ and $T_{m,j}$ [12]. By adding the fourth state, which is heat load related to occupants, we approximate the change of this state over time as constant [10]. The motivation for this arises from an assumption that occupant patterns, to some extent, are similar throughout the days. In this way, $q_{ig,j}$ is not an unmeasured input to the system anymore, but rather modeled as an additional state. To consider the multi-zone thermal building model, we evaluate the decentral approach, where no coupling between rooms or over the floor exists. Thus, each room is evaluated separately.

3.2 Parameter identification approach

To tackle the issue of thermal building models' robustness to occupant patterns, we propose the distinct consideration of two identification periods: the working days' identification period (5 days) and the weekend identification period (2 days). The incentive for this arises from the different occupant behavior patterns within commercial buildings during working days and weekends [15]. Separating the identification period can bring more accuracy and robustness to the model prediction, since the working-days-identified model learns occupants' patterns only during the working-days. In contrast, the weekend-identified model does not have the same occupant patterns, since weekends are non-working days and occupants dwell less in the building. Hence, they have a lower impact on indoor air temperature during these days. Considering a switch between the working-days-identified model and the weekend-identified model, fitting at the point of the switch is necessary. To make this transition smooth, the points between the prediction in the last two hours of the first model and the prediction of the first two

hours of the second model are linearly interpolated. To distinguish between the new approach proposed in the present paper which switches between two identified RC building models and the classically identified RC building model, the former will be named the *ensemble model*. Through the classical modeling approach, we identify the RC building model across the entire week period in a single instance, whereas the novelty of the new approach distinguishes the identification period of the forecasting models based on different patterns. In this case, we address the pattern of OB throughout the week and weekend separately. Thus, we define the ensemble model as a composition of two differently identified RC building models. Furthermore, it is possible to determine different patterns (e.g. seasons) and to use more than two differently identified RC building models in an ensemble model.

The proposed method and the workflow is depicted in Figure 2, whereas the subscripts *wd* and *we* refer to working days and weekend as identified parameters that are utilized in PMS (see Figure 1). Furthermore, the same structure of an RC building model depicted in Figure 1 is used for the classic and for the ensemble model approach to be able to compare the results qualitatively.

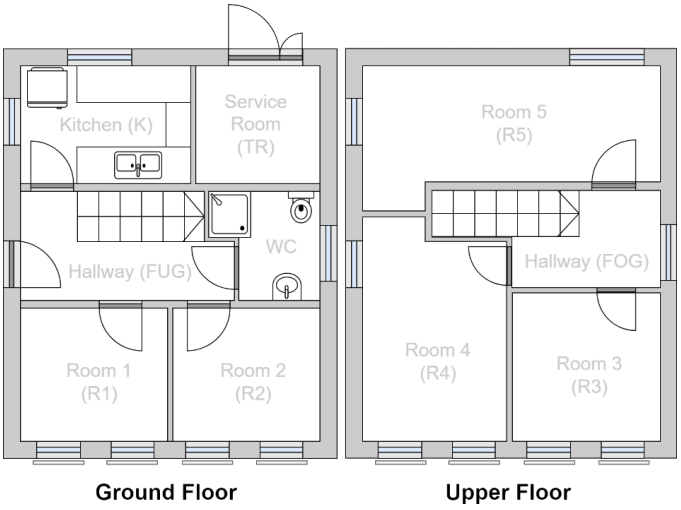

Figure 3: The plan of the Living Laboratory at Karlsruhe Institute of Technology [27].

4 EXPERIMENTAL RESULTS

The proposed methodology has been applied to the Living Laboratory on Campus North of the Karlsruhe Institute of Technology [17]. This building is used as a working space, where no information about occupant behavior is known. The building consists of five offices, a kitchen and a bathroom as shown in Figure 3. Hallways and service room are not considered in this study, since there is no heating available for these. Hence, the heat flow is measured for the whole building, we use Equation (6) to evaluate heating for each room. Besides heat flow, the ambient temperature, solar radiation, and indoor air temperature for each room are measured, too. The dataset covers the period from 23.09.2023 to 04.11.2023. The identification period for the week model is from 25.09.2023 midnight to 30.09.2023 midnight and for the weekend model from 23.09.2023 midnight to 25.09.2023 midnight. The rest of the data are used for validation of the model. We use a long-range validation period to prove the model structure's applicability over a longer period than one week. Due to the lack of measurement data in winter, the autumn period is chosen for this study, whereas the winter scenario needs further exploration. The identification and validation are undertaken using MATLAB System Identification Toolbox [31]. The previously described model is created as a state-space system, where the parameters inside the state matrix and input matrix are identified based on real data inputs. To show the convenience of the proposed model, we evaluate the methodology on a multi-zone model structure, where each room is presented as a single zone. This assumption is justified by Frahm et al. [15]. They showed that there is no significant difference between a multi-zone model with coupling over the floor and between rooms (centralized approach) and a multi-zone model without any coupling (decentralized approach). Thus, we use a multi-zone model with a decentralized approach.

Figure 4 shows indoor air temperature variation for room 4 during the validation period. The blue line presents measured indoor air temperature. The red and yellow lines present the forecasting results from the ensemble model and the classic model, respectively. To distinguish between weekends and working days, weekends are marked as grey-boxes. Measured data that are used as the input data are presented in the appendix of the present paper Figure 8.

5 EVALUATION

Each room is presented as a set of differential equations proposed in this paper, Equations (1)-(4). By dividing the model identification into working days and weekends, due to varying occupant behavior patterns, we achieve better indoor air temperature forecast as shown in Figure 4. In the first four days of the validation period, the introduced ensemble model overestimates indoor air temperature, whereas, for the rest of the validation period, it follows the dynamics of the system with better accuracy than the classic model. Considering the time-invariance of the state-space system, the classic model can not overcome unmeasured time-variant disturbances during the weekends 07.10.-08.10., 14.10.-15.10., 21.10.-22.10., 28.10.-29.10. and working days 16.10-20.10. and 30.10-03.11. On the other hand, the proposed ensemble structure, with its two identification models, demonstrates a higher capability to distinguish between weekends and working days forecasts.

5.1 Statistical indicators

To quantify the indoor air temperature prediction of the proposed ensemble model, we use the following statistical indicators: root-mean-square error (RMSE), [23], which is sensitive to outliers, the mean absolute error (MAE) [23], which denotes the average error between forecast and actual value and the mean absolute percentage error (MAPE) [25] which examines error as a percentage of the actual values. In Table 2 (see appendix), we present the error analysis of all three quantification methods, both for the identification period and validation period. Error indicators are shown for all rooms. It can be noted that during the validation period, according

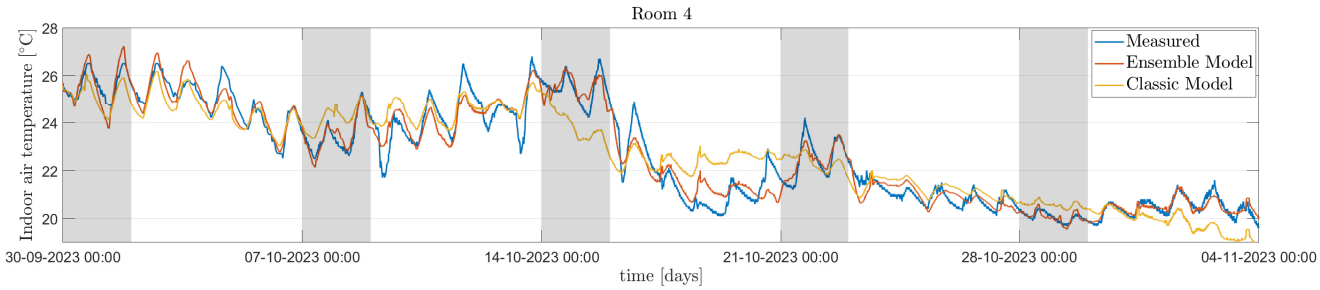

Figure 4: Comparison of the indoor air temperature prediction for room 4. Grey areas present weekend periods and white areas the working days.

to all three indicators, the ensemble model produces better predictions. MAPE of the ensemble model predictions is in the range of 1.4-2.8 %, while MAPE for the classic model is in the range of 2.9-5.3 %. MAE of both models are in the range of 0.32-0.53 °C and 0.65-1.13 °C, respectively, while RMSE is slightly higher for both models since it penalizes outliers, 0.43-0.89 °C and 0.84-1.41 °C, respectively. The least favorable performance of both algorithms is for the bathroom, due to the significant impact of unmeasured disturbances which affect a fast decrease of the indoor air temperature (see appendix, Figure 9). Both model algorithms can not capture these fast system dynamics. During the identification period, the performance of the classic model forecast is superior only for room 5, while for all other zones the ensemble model achieves a better forecast. During the validation period, the ensemble model has a lower error forecast for all zones. Interestingly, when observing room 5, the indoor air temperature forecast of the ensemble has the lowest error when compared with other zones during the validation period, even though during the identification period the classic model forecast of room 5 is more convenient.

5.2 Distribution of prediction residuals

In addition to statistical indicators, the distribution of prediction residuals is analyzed. For all rooms and both models histograms are created, and the distributions are compared with the Euclidean norm, for all rooms within each model class and between the models. Histograms in Figure 5 show the error distribution for the classic and ensemble models for all zones, respectively. The error distributions are not systematic errors, but stochastic errors that depend on the weather and occupancy. It can be noted that the proposed ensemble model prediction leads to a better fit to a normal distribution than the classic model in all seven cases. When comparing the histograms for room 4, the spectrum where 95 % of the residuals for the classic model lies, is from -1.77 to 1.77, whereas for the ensemble model is narrower from -0.89 to 0.89, denoting that 95 % of errors between prediction and real indoor air temperature is less than or equal to 0.89 °C. Standard deviations of the classic and ensemble forecast are 0.91 °C and 0.46 °C, respectively. Whereas mean values are for both near to zero. A smaller standard deviation denotes that the error is closer to the mean value, indicating higher precision of forecast.

To compare the histograms, we define a similarity index based on the Euclidean norm. Figure 10, presented in the appendix, depicts

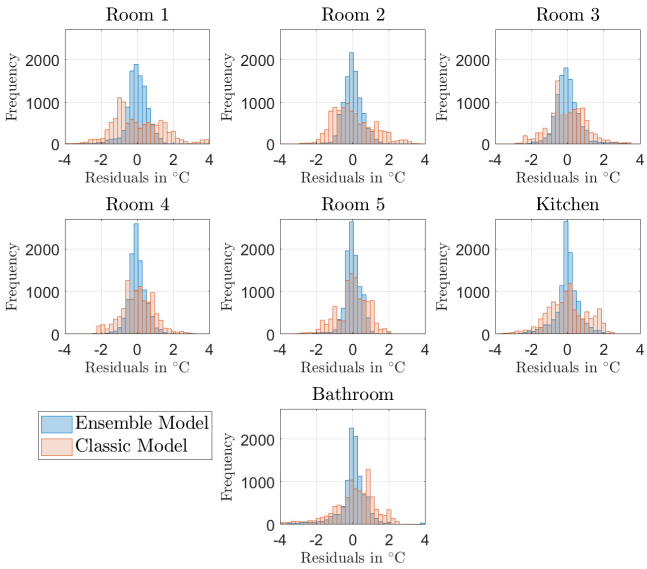

Figure 5: Comparison of the residual histograms of classic and ensemble model for all zones.

the similarity of the distributions using the Euclidean norm when comparing histograms of all rooms and models against each other. For this purpose, EM_i denotes the histogram of the ensemble models and CM_i histogram of the classic model structures. It is obvious that the distance matrix in Figure 10 is symmetrical and excludes self-similarity. In general, there is a high similarity of the distribution of the histograms within each ensemble model (EM_i, EM_j) and the classic model (CM_i, CM_j). Furthermore, it can be observed that the distributions between the models show the highest discrepancy (EM_i, CM_j). In detail, the smallest distances between histograms are in the first quarter of the plot where histograms of the ensemble method are compared (EM_i, EM_j), with a minimum of 363, maximum of 1303, average of 785 and median of 884. As expected, the largest distances are in the second (EM_i, CM_j) and third quarters (CM_i, EM_j), where the two different models are compared, with a minimum of 1395, maximum of 3510, average of 2284 and median of 2237. The fourth quarter (CM_i, CM_j) presents a comparison of histograms for classic model structures denoting the similarity of

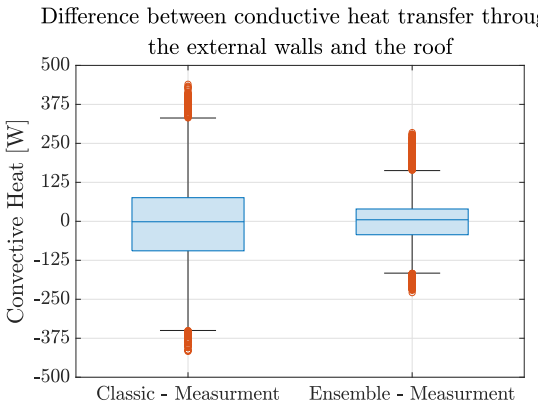

Figure 6: Difference between conductive heat transfer of measurement data and both forecasts through the external walls and the roof summed for all zones.

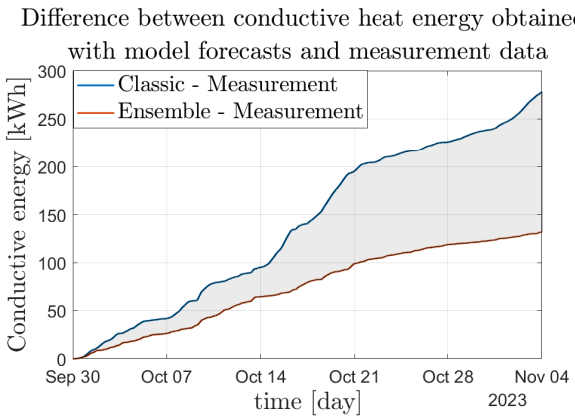

Figure 7: Difference of conductive energy between measurement data and both forecasts through the external walls and the roof summed for all zones. The introduced novel method reduces building energy consumption for 146 kWh during the five experimental weeks.

the error for each zone with a minimum of 685, maximum of 1972, average of 1148 and median of 1290. When comparing the first and fourth quarters, it can be concluded that the first has an overall smaller Euclidean norm.

5.3 Evaluation of transmission heat energy gain and loss through walls and roof

Based on the analysis of the indoor air temperature forecasts, we quantitatively assess the transmission energy gain and loss through external walls and the roof for all zones. Transmission heat gain and loss through a building envelope consists of three components i.e. conduction, convection and radiation. Since the transmission heat gain and loss are calculated in each time step, the effects of convection and radiation are negligible. Therefore, we use Fourier's Law directly in Equation (7) to calculate the conductive heat gain and loss through all zones for each time interval, where k [W/(mK)] is the thermal conductivity, A [m^2] is the surface area of walls and roofs, and d [m] is the thickness. The temperature difference between indoor air and ambient is represented by ΔT.

$$Q_{cond} = \frac{k \cdot A \cdot \Delta T}{d} \tag{7}$$

Figure 6 visualizes the difference between conductive heat power obtained with measurement data and classic model forecast (left) and measurement data and ensemble model forecast (right) in each time step. The box charts depict upper and lower quartiles with median, minimum and maximum values excluding outliers that are shown separately as red circles and are calculated using the interquartile range (IQR). The IQR of the difference between conductive heat power obtained with the forecast of the ensemble model and measurement data is in the range of -43 W to 40 W, whereas that of the classic model is in the range of -95 W to 76 W. Heat losses are presented with a positive sign and heat gains with a negative sign. Furthermore, the accumulated prediction error over the whole period in heat energy gain and loss between models and measurement are presented in Figure 7. In this, the difference between heat energy calculated with the classic model and measurement data over five weeks is 278 kWh, whereas the difference between energy calculated with the ensemble model and measurement data is 132 kWh. The results confirm that the ensemble model has greatly improved the accuracy of the prediction and thus minimized the accumulated error of heat energy gain and loss transmitted through external walls and roof.

6 DISCUSSION

Low deviation between error indicators MAE and RMSE show consistent performance of both model approaches, without individual outliers with high prediction error. However, all three statistical indicators in Table 2 show that the forecast error of the ensemble model is lower than that of the classic model for all rooms during the validation period. Nevertheless, comparing residual histograms in Figure 5, results show that the range of residuals of the ensemble model is narrower than for the classic model, clarifying that the ensemble model performs better. By comparing the ensemble model and classic model in the heatmap-matrix in Figure 10 (see appendix), it can be concluded that the ensemble model structure is more robust to the change of zones i.e. different datasets and different unmeasured disturbances, e.g. occupant-related heat load which directly affects the indoor air temperature of the corresponding zone. In addition, conductive heat transfer of measurement data and both models are also indicators of model accuracy. Figure 6 shows the difference between measurement and both forecasts in conductive energy through external walls and roof. The IQR of the difference between heat power obtained with the forecast of the ensemble model and measurement data is in a much smaller range than that of the classic model. Therefore, it can be concluded that the conductive heat power calculation with the ensemble model is much more accurate than that with the classic model. Conductive heat energy is presented in Figure 7, where it can be concluded that the ensemble model reduces the error of conductive heat energy for 146 kWh over five experimental weeks.

We can not directly compare the performance of the proposed grey-box model with already existing models in the literature in Table 1, since each method uses different data and other time horizons for identification and validation periods. Harb et al. [18] developed a 4R3C model with an RMSE of 0.2, whereas they use an identification period of 26 days. Frahm et al. [15] showed that, to some extent, the two-day identified model can achieve a good forecast. In contrast, Gray et al. [16] and Klanatsky et al. [26] update the parameter on a daily/weekly basis and use 1-4 weeks for identification, thus they achieved an RMSE of 0.2 and an MAE of 0.25 over the year, respectively. We decompose the identification period into weekend and weekdays to achieve a more robust model for different occupation patterns. We demonstrate that one week of parameter identification is sufficient for accurate forecasting of indoor air temperature for the subsequent five weeks. To enable a direct comparison, we develop a classic model for identification on a whole week period (23.09.2023-30.09.2023). With the proposed model, we achieve a relative mean MAPE reduction of 2.32 % over the validation period compared to the forecast of the classic model. Thus, we demonstrate the superiority of the proposed ensemble model for high-accuracy forecasting.

However, the ensemble model overestimates the indoor air temperature in room 4 during the first four days, see Figure 4, which happens due to significant changes in ambient temperature and heat pump operation, which is mostly turned off. Therefore, the validation is not optimal for this period. Additionally, in the bathroom fast temperature drops exist Figure 9, which represent unmeasured disturbances. The ensemble model can not capture these fast dynamics of the system and predict temperature minimums throughout the days. Interestingly, during the identification period the classic model of room 5 achieves a better forecast and during the validation period ensemble model of room 5 has favorable performances (see Table 2 in appendix). During the identification period, fast temperature drops in room 5 appear, which can lead to higher inaccuracies in the forecasting, similar to the indoor air temperature forecast in the bathroom. Additionally, room 5 faces northwest, where the solar radiation has the smallest impact and where occupant patterns could be more complex since it is the largest room in the building.

7 CONCLUSION

This paper presents a new approach for grey-box building models that are more robust to occupant-related heat load. The performance of grey-box thermal building models plays an important role in model-based control systems, where better prediction can lead to more effective building energy control. Due to different occupant behavior patterns and their impact on indoor air temperature (i.e. occupant-related heat load) in commercial buildings, we introduce an ensemble model that distinguishes between weekend and working days models to get more precise and more robust predictions. Therefore, two identification periods are used, working days (five-day identification period) and weekend identification period (two-day identification period). In this way, we develop two models with the same structure but different estimated parameters. Furthermore, we obtain more accurate forecasts throughout five validation weeks, with minimal additional effort but deliver significantly better results. The new approach is extended and verified on a decentralized multi-zone building, where ambient air temperature, solar radiation, heat flow of the heat pump and indoor air temperature of each room are real data, that are used for parameter identification. The proposed model is compared with the classic model, where the parameters are identified on the range of the whole week. Findings reveal that the proposed ensemble model has more accurate prediction over the validation period than the classic model. The ensemble model still can not predict fast dynamics of the system such as temperature drop in the bathroom. The overestimation of indoor air temperature in room 4, at the beginning of the validation period, and additional impacts on forecast of the room 5 during the identification period need to be further investigated and should be reduced.

Several avenues for future work exist. Since the introduced study is undertaken within the autumn period, due to the lack of other measurement data, further evaluations considering heating and cooling seasons are necessary. The ensemble model for the whole year period should be investigated, where the minimal number of models (i.e. winter and summer models, models for vacation periods) inside an ensemble should be explored. This work uses the same grey-box model structure for the weekend and week models, whereas research on second and third-order systems needs to be done. Simplified models could accurately represent weekends where occupants don't have a great impact on indoor air temperature. Reduction of order in the state-space system can have a significant impact since the multi-zone model is utilized. Furthermore, occupancy behavior for non-commercial buildings should be investigated, where ensemble structure might differ and have a smaller or bigger impact.

ACKNOWLEDGMENTS

This work was conducted within the framework of the Helmholtz Program Energy System Design (ESD).

REFERENCES

[1] Zakia Afroz, GM Shafiullah, Tania Urmee, and Gary Higgins. 2018. Modeling techniques used in building HVAC control systems: A review. *Renewable and sustainable energy reviews* 83 (2018), 64–84.

[2] Krzysztof Arendt, Muhyiddine Jradi, Hamid Reza Shaker, and Christian Veje. 2018. Comparative analysis of white-, gray-and black-box models for thermal simulation of indoor environment: Teaching building case study. In *Proceedings of the 2018 Building Performance Modeling Conference and SimBuild co-organized by ASHRAE and IBPSA-USA, Chicago, IL, USA*. 26–28.

[3] Gaby Baasch, Paul Westermann, and Ralph Evins. 2021. Identifying whole-building heat loss coefficient from heterogeneous sensor data: An empirical survey of gray and black box approaches. *Energy and Buildings* 241 (2021), 110889.

[4] Peder Bacher and Henrik Madsen. 2011. Identifying suitable models for the heat dynamics of buildings. *Energy and buildings* 43, 7 (2011), 1511–1522.

[5] Yasaman Balali, Adrian Chong, Andrew Busch, and Steven O'Keefe. 2023. Energy modelling and control of building heating and cooling systems with data-driven and hybrid models—A review. *Renewable and Sustainable Energy Reviews* 183 (2023), 113496.

[6] Walid Belazi, Salah-Eddine Ouldboukhitine, Alaa Chateauneuf, and Abdelhamid Bouchair. 2018. Uncertainty analysis of occupant behavior and building envelope materials in office building performance simulation. *Journal of Building Engineering* 19 (2018), 434–448.

[7] Max Bird, Camille Daveau, Edward O'Dwyer, Salvador Acha, and Nilay Shah. 2022. Real-world implementation and cost of a cloud-based MPC retrofit for HVAC control systems in commercial buildings. *Energy and Buildings* 270 (2022), 112269.

[8] Thea Hauge Broholt, Michael Dahl Knudsen, and Steffen Petersen. 2022. The robustness of black and grey-box models of thermal building behaviour against weather changes. *Energy and Buildings* 275 (2022), 112460.

[9] Jiří Cígler, Dimitrios Gyalistras, Jan Široky, V Tiet, and Lukaš Ferkl. 2013. Beyond theory: the challenge of implementing model predictive control in buildings. In *Proceedings of 11th Rehva world congress, Clima*, Vol. 250.
[10] Austin R Coffman and Prabir Barooah. 2018. Simultaneous identification of dynamic model and occupant-induced disturbance for commercial buildings. *Building and Environment* 128 (2018), 153–160.
[11] Borui Cui, Cheng Fan, Jeffrey Munk, Ning Mao, Fu Xiao, Jin Dong, and Teja Kuruganti. 2019. A hybrid building thermal modeling approach for predicting temperatures in typical, detached, two-story houses. *Applied energy* 236 (2019), 101–116.
[12] Roel De Coninck, Fredrik Magnusson, Johan Åkesson, and Lieve Helsen. 2016. Toolbox for development and validation of grey-box building models for forecasting and control. *Journal of building performance simulation* 9, 3 (2016), 288–303.
[13] Ján Drgoňa, Javier Arroyo, Iago Cupeiro Figueroa, David Blum, Krzysztof Arendt, Donghun Kim, Enric Perarnau Ollé, Juraj Oravec, Michael Wetter, Draguna L Vrabie, et al. 2020. All you need to know about model predictive control for buildings. *Annual Reviews in Control* 50 (2020), 190–232.
[14] Moritz Frahm, Felix Langner, Philipp Zwickel, Jörg Matthes, Ralf Mikut, and Veit Hagenmeyer. 2022. How to Derive and Implement a Minimalistic RC Model from Thermodynamics for the Control of Thermal Parameters for Assuring Thermal Comfort in Buildings. In *2022 Open Source Modelling and Simulation of Energy Systems (OSMSES)*. IEEE, 1–6.
[15] Moritz Frahm, Stefan Meisenbacher, Elena Klumpp, Ralf Mikut, Jörg Matthes, and Veit Hagenmeyer. 2022. Multi-zone grey-box thermal building identification with real occupants. In *Proceedings of the 9th ACM International Conference on Systems for Energy-Efficient Buildings, Cities, and Transportation*. 484–487.
[16] Francesco Massa Gray and Michael Schmidt. 2018. A hybrid approach to thermal building modelling using a combination of Gaussian processes and grey-box models. *Energy and Buildings* 165 (2018), 56–63.
[17] Veit Hagenmeyer, Hüseyin Kemal Çakmak, Clemens Düpmeier, Timm Faulwasser, Jörg Isele, Hubert B Keller, Peter Kohlhepp, Uwe Kühnapfel, Uwe Stucky, Simon Waczowicz, et al. 2016. Information and communication technology in energy lab 2.0: Smart energies system simulation and control center with an open-street-map-based power flow simulation example. *Energy Technology* 4, 1 (2016), 145–162.
[18] Hassan Harb, Neven Boyanov, Luis Hernandez, Rita Streblow, and Dirk Müller. 2016. Development and validation of grey-box models for forecasting the thermal response of occupied buildings. *Energy and Buildings* 117 (2016), 199–207.
[19] Rasmus Elbæk Hedegaard and Steffen Petersen. 2017. Evaluation of grey-box model parameter estimates intended for thermal characterization of buildings. *Energy Procedia* 132 (2017), 982–987.
[20] Tianzhen Hong, Da Yan, Simona D'Oca, and Chien-fei Chen. 2017. Ten questions concerning occupant behavior in buildings: The big picture. *Building and Environment* 114 (2017), 518–530.
[21] IEA. 2023. Renewables. https://www.iea.org/reports/tracking-clean-energy-progress-2023. Accessed: 06.12.2023.
[22] Z Jiang, Q Chen, and A Moser. 1992. Indoor airflow with cooling panel and radiative/convective heat source. (1992).
[23] Dulakshi Santhusitha Kumari Karunasingha. 2022. Root mean square error or mean absolute error? Use their ratio as well. *Information Sciences* 585 (2022), 609–629.
[24] Miroslava Kavgic, Trent Hilliard, and Lukas Swan. 2015. Opportunities for implementation of MPC in commercial buildings. *Energy Procedia* 78 (2015), 2148–2153.
[25] Ummul Khair, Hasanul Fahmi, Sarudin Al Hakim, and Robbi Rahim. 2017. Forecasting error calculation with mean absolute deviation and mean absolute percentage error. In *journal of physics: conference series*, Vol. 930. IOP Publishing, 012002.
[26] Peter Klanatsky, François Veynandt, and Christian Heschl. 2023. Grey-box model for model predictive control of buildings. *Energy and Buildings* 300 (2023), 113624.
[27] Chang Li, Kevin Förderer, Tobias Moser, Luigi Spatafora, and Veit Hagenmeyer. 2024. Gossen's First Law in the Modeling for Demand Side Management: A First Heat Pump Case Study. In *Energy Informatics*, Bo Nørregaard Jørgensen, Luiz Carlos Pereira da Silva, and Zheng Ma (Eds.). Springer Nature Switzerland, Cham, 111–125.
[28] Yanfei Li, Zheng O'Neill, Liang Zhang, Jianli Chen, Piljae Im, and Jason DeGraw. 2021. Grey-box modeling and application for building energy simulations-A critical review. *Renewable and Sustainable Energy Reviews* 146 (2021), 111174.
[29] Piotr Michalak. 2017. The development and validation of the linear time varying Simulink-based model for the dynamic simulation of the thermal performance of buildings. *Energy and Buildings* 141 (2017), 333–340.
[30] Maarten Sourbron, Clara Verhelst, and Lieve Helsen. 2013. Building models for model predictive control of office buildings with concrete core activation. *Journal of building performance simulation* 6, 3 (2013), 175–198.
[31] The MathWorks Inc. [n. d.]. *System Identification Toolbox: 9.16 (R2022a)*. https://www.mathworks.com
[32] Xiang Zhang, Christoffer Rasmussen, Dirk Saelens, and Staf Roels. 2022. Time-dependent solar aperture estimation of a building: Comparing grey-box and white-box approaches. *Renewable and Sustainable Energy Reviews* 161 (2022), 112337.

APPENDIX

Evaluation data

Figure 8 shows weather data consisting of ambient temperature and solar radiation (top) and the heat flow from the heat pump for the corresponding room (bottom).

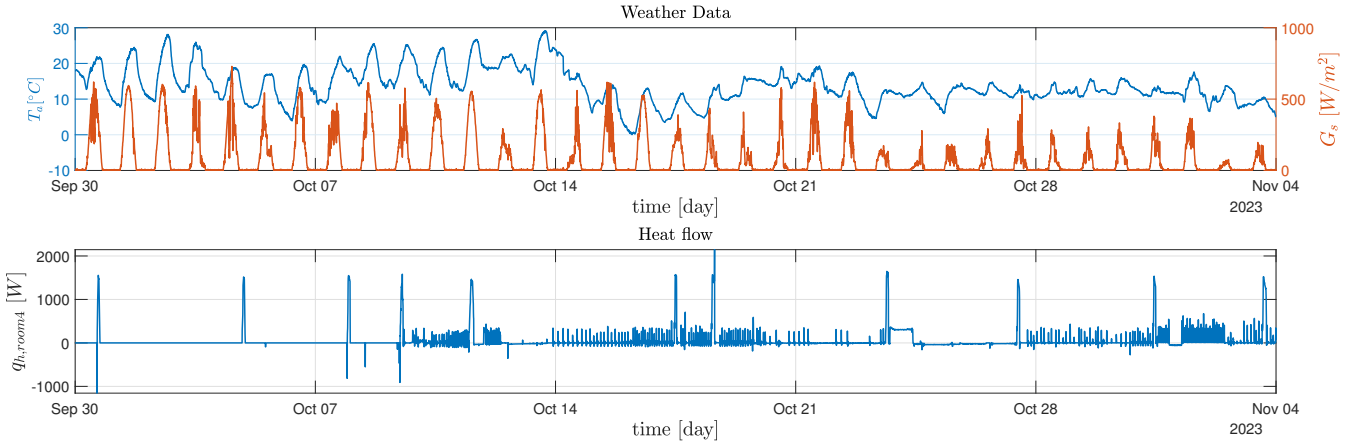

Figure 8: Input data for room 4: ambient temperature and solar radiation (top) and heat flow (bottom).

Indoor air temperature forecast

Figure 9 shows the indoor air temperature in the bathroom over the validation period. The blue, red and yellow lines show the measured indoor air temperature, the prediction results of the ensemble model and the prediction results of the classic model, respectively. The weekends are shown as grey boxes.

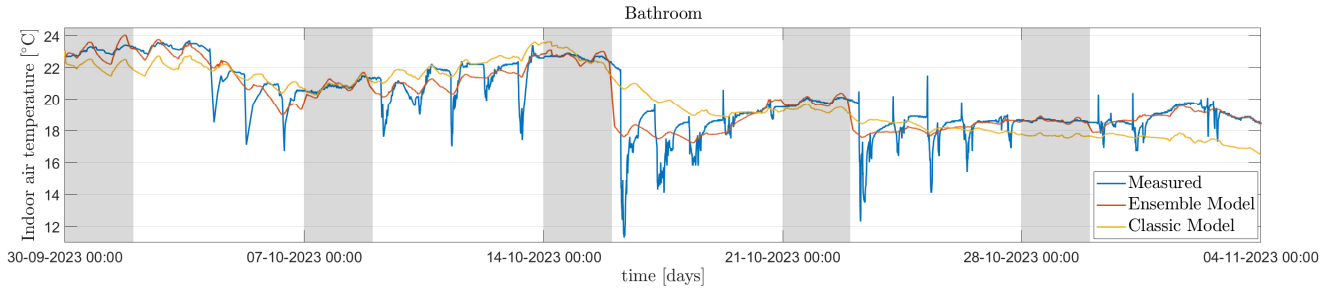

Figure 9: Comparison of the indoor air temperature prediction for the bathroom. Grey areas present weekend periods and white areas working days.

Error analysis for all seven zones

Table 2 shows the MAE, RMSE and MAPE for classic and ensemble models over the identification and validation period for all zones.

Table 2: Indoor air temperature error analysis for all zones

		MAE [°C]	RMSE [°C]	MAPE [%]	MAE [°C]	RMSE [°C]	MAPE [%]
Zone	Algorithm	Identification period			Validation period		
Room 1	Classic	0.3549	0.4145	1.3840	1.1311	1.3774	5.0135
	Ensemble	0.2550	0.3098	0.9995	0.4247	0.5842	1.9082
Room 2	Classic	0.4469	0.5606	1.7427	0.8928	1.1046	3.7803
	Ensemble	0.4196	0.5431	1.6526	0.3912	0.5026	1.6710
Room 3	Classic	0.6363	0.8305	2.5114	0.8065	1.0126	3.6309
	Ensemble	0.4658	0.5915	1.8482	0.4684	0.6421	2.0650
Room 4	Classic	0.4747	0.5514	1.8675	0.7139	0.9051	3.1753
	Ensemble	0.3482	0.4150	1.3769	0.3463	0.4576	1.5125
Room 5	Classic	0.3864	0.5028	1.5842	0.6529	0.8446	2.9213
	Ensemble	0.4121	0.5200	1.6906	0.3219	0.4282	1.4230
Kitchen	Classic	0.5604	0.7593	2.2440	0.8727	1.1015	3.7413
	Ensemble	0.5277	0.7445	2.1086	0.4349	0.6315	1.8676
Bathroom	Classic	0.7293	1.1242	3.5351	0.9972	1.4081	5.3254
	Ensemble	0.6939	1.0876	3.3665	0.5307	0.8856	2.8292

Comparison of the ensemble and classic model in the heatmap-matrix

Figure 10 shows the similarity of the distributions of the prediction residuals established on the Euclidean norm. The distributions of all zones and models are compared with each other. The EM_i represents the histogram of the ensemble models and the CM_i histogram of the classical model structures.

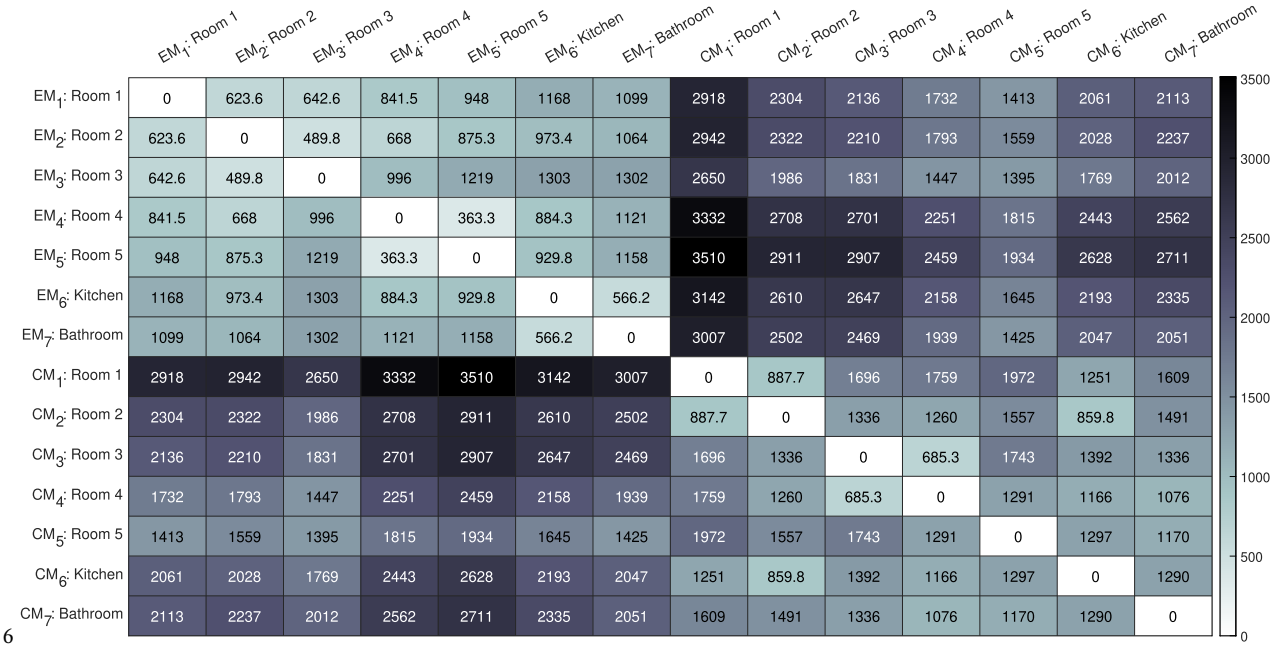

Figure 10: Similarity indices of the histograms of two models across all zones. EM denotes the histogram of the ensemble models and CM the histograms of the classic model structures.